

Path Following for Formations of Underactuated Marine Vessels under Influence of Constant Ocean Currents

D.J.W. Belleter and K.Y. Pettersen

Abstract—In this paper the straight line path following problem is considered for formations of underactuated marine vessels. The vessels are affected by a constant ocean current that is bounded, and irrotational with respect to the inertial frame. A Line-of-Sight (LOS) guidance law with two feedback linearising controllers is used to achieve path following of each individual vessel. Integral action is added to the LOS guidance law to compensate the effects of the ocean current acting on each vessel. In addition to the individual geometric task of path convergence, the vessels must also achieve the formation control task. More specifically, the vessels have to move along the desired path with a specified relative inter-vessel distance and with a constant desired velocity. This task is accomplished using a nonlinear formation control law. The closed-loop dynamics are analysed using theory for feedback-interconnected cascaded systems. It is shown that the origin of the closed-loop error dynamics of the combined path following dynamics and formation dynamics is uniformly globally asymptotically stable. Simulation results are presented in a case study.

I. INTRODUCTION

Control of systems consisting of multiple agents has been a topic of active research in the control community in recent years. The motivation for using multi-agents systems is that they can perform tasks more time efficiently and cost effectively than a single, often more complex, vehicle. Moreover, the financial and operational consequences of vehicle loss in inaccessible environments, such as deep sea or under ice, are less. Coordinated path following for multi-agent systems is valuable especially for information gathering tasks, where the formations can be used to cover a larger area simultaneously than single vehicles would.

The path following control problem for marine vehicles is a well studied problem, see for instance [1]–[9]. Both in practice and in the control research literature Line-of-Sight (LOS) guidance is a popular choice to solve the path following problem. When using LOS guidance, robustness against ocean currents needs to be considered to ensure good performance of the controllers. In particular, if the currents are not considered, LOS guidance will not give convergence to the desired path, but will give a constant deviation dependent on the magnitude of the current. To compensate for the effects of the ocean currents, adaptive control methods are proposed in [10], while integral action is added to the LOS guidance law in [11]–[13]. However, these works all consider single vehicles.

Cooperative control of multi-agent systems has been the focus of a number of different recent works, see for instance [14] and [15]. The problem of path following control of formations of marine vehicles is studied in [16]–[21]. In [19] path following of two underwater vehicles is investigated. The vehicles follow parallel paths, whilst achieving and maintaining a desired along-path distance. In [20], [21] coordinated path following in the presence of

This work was partly supported by the Research Council of Norway through its Centres of Excellence funding scheme, project No. 223254 AMOS.

D.J.W. Belleter and K.Y. Pettersen are with the Centre for Autonomous Marine Operations and Systems (AMOS) and the Department of Engineering Cybernetics, Norwegian University of Science and Technology, NO7491 Trondheim, Norway {dennis.belleter,kristin.y.pettersen}@itk.ntnu.no.

communication failures and time delays is considered. In [16]–[18] straight-line path following for formations of marine vehicles is considered. In particular, in [16]–[18] LOS guidance is used to make each vehicle in the formation follow a desired path, whilst a formation control term is added to the velocity control to achieve a desired inter-agent distance and formation. However, in all the formation control approaches discussed above the effects of ocean currents are not taken into account. Ocean current are considered in for instance [22], [23], however these works consider fully actuated marine vehicles. In [24] formation control of underactuated vessels under the influence of constant disturbances is considered using neural network adaptive dynamic surface control, which also takes into account modelling uncertainties but results in more complicated control laws than the approach taken here. In [25] LOS with a conditional integrator is used for path following under the influence of unknown disturbances, however this approach requires estimates of the current.

This paper aims to unify the results for integral LOS path following of underactuated marine vessels in the presence of ocean currents from [11] and [13], with LOS path following results for formations of underactuated marine vessels from [18], in order to achieve path following control of formations of underactuated marine vessels in a two dimensional plane that also takes into account the ocean currents.

Motivated by [11], [13], and [18] we use a cascaded systems approach. It is interesting to note that the combination of the integral LOS guidance control, which has adaptive properties, together with the formation keeping control, introduces a feedback-loop in the system that is not present when only one of these features is present in the system. The approach of cascaded control used in [11], [13], and [18] can therefore not be directly applied. In particular, the combination of adaption and formation keeping makes it necessary to “break the loop” [26]. Using this approach, we prove that the origin of the closed-loop error dynamics is uniformly globally asymptotically stable (UGAS).

The paper is organized as follows. In Section II the model of an underactuated surface vessel is given and the control objectives are stated. In Section III the controllers to solve the control problem are presented and the main result is stated. Section IV contains the proof of the main theoretical result. A case study is presented in Section V. Finally Section VI gives the conclusions of the work and a discussion of future work.

II. VESSEL MODEL AND CONTROL OBJECTIVE

A. The Vessel Model

The motion of marine vessels in the horizontal plane is described by the position and orientation of the vessel w.r.t. the inertial frame i , i.e. the state vector is given by $\mathbf{p} \triangleq [x, y, \psi]$. The corresponding vector of linear and angular velocities is given by $\mathbf{v} \triangleq [u, v, r]^T$, containing the surge velocity u , sway velocity v , and yaw rate r .

The ocean current, expressed in the inertial frame i , is denoted by \mathbf{V}_c and satisfies the following assumption.

Assumption 1: The ocean current is assumed to be constant and irrotational w.r.t. i , i.e. $\mathbf{V}_c \triangleq [V_x, V_y, 0]^T$. Furthermore, it is bounded by $V_{\max} > 0$ such that $\|\mathbf{V}_c\| = \sqrt{V_x^2 + V_y^2} \leq V_{\max}$. The velocity of the ocean current expressed in the body-fixed frame b , $\mathbf{v}_{cr} \triangleq [u_{cr}, v_{cr}, 0]^T$, can be obtained by $\mathbf{v}_{cr} = \mathbf{R}^T(\psi)\mathbf{V}_c$, where $\mathbf{R}(\psi)$ is the rotation matrix from b to i defined as

$$\mathbf{R}(\psi) \triangleq \begin{bmatrix} \cos(\psi) & -\sin(\psi) & 0 \\ \sin(\psi) & \cos(\psi) & 0 \\ 0 & 0 & 1 \end{bmatrix}. \quad (1)$$

As in [13] the model is defined in terms of the relative velocity expressed in b , defined as $\mathbf{v}_r \triangleq \mathbf{v} - \mathbf{v}_{cr} = [u_r, v_r, r]^T$. Since the ocean current is irrotational, surface vessels, and also underwater vehicles moving in the horizontal plane, are described by the 3-DOF manoeuvring model from [27]:

$$\dot{\mathbf{p}} = \mathbf{R}(\psi)\mathbf{v}_r + [V_x, V_y, 0]^T \quad (2)$$

$$\mathbf{M}\dot{\mathbf{v}}_r + \mathbf{C}(\mathbf{v}_r)\mathbf{v}_r + \mathbf{D}\mathbf{v}_r = \mathbf{B}\mathbf{f}. \quad (3)$$

The vector $\mathbf{f} \triangleq [T_u, T_r]^T$ is the control input vector, containing the surge thrust T_u and the rudder angle T_r . The matrix $\mathbf{M} = \mathbf{M}^T > 0$ is the system inertia matrix including added mass, \mathbf{C} is the Coriolis and centripetal matrix, \mathbf{D} is the hydrodynamic damping matrix, and \mathbf{B} is the actuator configuration matrix.

Assumption 2: We assume port-starboard symmetry.

Remark 1: Assumption 2 is to the authors' best knowledge satisfied for all commercial surface and underwater vessels.

The matrices \mathbf{M} , \mathbf{D} , and \mathbf{B} are defined as

$$\mathbf{M} \triangleq \begin{bmatrix} m_{11} & 0 & 0 \\ 0 & m_{22} & m_{23} \\ 0 & m_{23} & m_{33} \end{bmatrix}, \mathbf{D} \triangleq \begin{bmatrix} d_{11} & 0 & 0 \\ 0 & d_{22} & d_{23} \\ 0 & d_{23} & d_{33} \end{bmatrix}, \mathbf{B} \triangleq \begin{bmatrix} b_{11} & 0 \\ 0 & b_{22} \\ 0 & b_{32} \end{bmatrix},$$

and \mathbf{C} can be derived from \mathbf{M} (See [27]). Since \mathbf{M} is positive definite, and the damping is dissipative, the constant $d_{11}/m_{11} > 0$. For the special case of underwater vehicles moving in the horizontal plane, the matrices \mathbf{M} and \mathbf{D} will typically be diagonal.

The model can be written in component form as

$$\dot{x} = u_r \cos(\psi) - v_r \sin(\psi) + V_x, \quad (4a)$$

$$\dot{y} = u_r \sin(\psi) + v_r \cos(\psi) + V_y, \quad (4b)$$

$$\dot{\psi} = r, \quad (4c)$$

$$\dot{u}_r = F_{u_r}(v_r, r) - \frac{d_{11}}{m_{11}}u_r + \tau_u, \quad (4d)$$

$$\dot{v}_r = X(u_r)r + Y(u_r)v_r, \quad (4e)$$

$$\dot{r} = F_r(u_r, v_r, r) + \tau_r, \quad (4f)$$

the position of the body-fixed frame is chosen such that $\mathbf{M}^{-1}\mathbf{B}\mathbf{f} = [\tau_u, 0, \tau_r]$. This is possible as long as the original position of the body-fixed frame is located along the centreline of the vessel. Coordinate transformations for this translation can be found in [4]. The definitions of F_{u_r} , $X(u_r)$, $Y(u_r)$, and F_r are given in Appendix I. Note that $X(u_r)$ and $Y(u_r)$ are bounded for bounded arguments and $Y(u_r)$ satisfies the following assumption.

Assumption 3: It is assumed that $Y(u_r)$ satisfies

$$Y(u_r) \leq -Y_{\min} < 0, \forall u_r \in [-V_{\max} - a, U_{rd} + a],$$

with a a parameter of the formation control law to be defined later.

Remark 2: This assumption is satisfied for commercial vessels by design, since $Y(u_r) \geq 0$ would imply an undamped or nominally unstable vessel is sway direction.

B. The Control Objectives

The goal is to have a formation of n vessels follow a desired straight line path \mathcal{P} . The vessels should move along this path with a desired constant relative surge velocity $U_{rd} > 0$ w.r.t. b . The

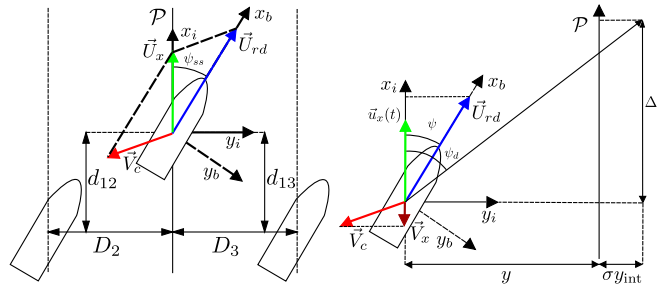


Fig. 1. The desired formation.

Fig. 2. Integral LOS guidance.

desired formation is illustrated in Fig. 1. The control objectives are to be achieved by decentralized controllers, i.e. each vessel will compute the required control action for convergence to the path and to achieve the desired velocity, based on measurements of own position and relative distances. The inertial frame is chosen such that its x -axis is aligned with the desired path, and consequently $\mathcal{P} \triangleq \{(x, y) \in \mathbb{R}^2 : y = 0\}$. The desired position of the j th vessel in the formation can then be described by the distance to the path D_j and by a relative distance between agent i and j along the path d_{ji} as shown in [18]. This results in the control objectives:

$$\lim_{t \rightarrow \infty} y_j(t) - D_j = 0, \quad (5)$$

$$\lim_{t \rightarrow \infty} \psi_j(t) = \psi_{ss}, \quad \psi_{ss} \in \left(-\frac{\pi}{2}, \frac{\pi}{2}\right), \quad (6)$$

$$\lim_{t \rightarrow \infty} u_{rj}(t) - U_{rd} = 0, \quad (7)$$

$$\lim_{t \rightarrow \infty} x_j(t) - x_i(t) - d_{ji} = 0, \quad (8)$$

for $j, i = 1, \dots, n$. It should be noted that the yaw angle should not converge to zero but rather to a constant value. This constant side-slip angle is required for the vessels to keep a straight line path in the presence of ocean currents, since the vessels are not actuated in sway. Finally the following assumption is made for the velocity.

Assumption 4: It is assumed that $V_{\max} + a < U_{rd} < U_{\max} - a$ where U_{\max} is the maximum attainable surge velocity of the vessel.

Remark 3: Assumption 4 requires that the vessel can achieve a relative surge speed higher than the sum of the maximum of the current and some additional freedom in the velocity used for the formation control. In general, Assumption 4 is easily satisfied since propulsion systems are designed to achieve much higher relative surge velocities than the velocity of the ocean current usually is.

The control objectives (5)-(8) show that the problem can be divided into two parts. Objectives (5) and (6) are individual path following control goals to ensure convergence to the path and a steady-state side-slip angle to compensate for the effect of the current. Objectives (7) and (8) are formation control goals that specify that the vessels keep a specified inter-vessel distance and move along the path whilst keeping a desired relative surge velocity.

C. Vessel Communication Network

The control objective (8) is defined in terms of the along-path position of multiple vessels. Hence, the vessels need to communicate their along-path position. Graph theory (see for instance [28]) is used to describe the communication.

The communication network is represented by a directed graph or digraph $\mathcal{G}(V, E)$, where V is a set of vertices and E a set of edges. The vertices represent the vessels in the formation and the number of vertices is equal to the number of vessels. The edges represent communication channels and are represented by pairs of vertices. More specifically, if there is information transfer from vertex v_i to v_j then the pair $(v_j, v_i) \in E$.

The neighbourhood \mathcal{A}_j of v_j is the set of vertices $v_i \in V$ such that there is an edge from v_j to v_i . Hence, when controlling vessel j only the along-path position x_i of the vessels where $i \in \mathcal{A}_j$ may be used. The above allows us to give some definitions, based on [29], that are used in the analysis of the formation dynamics. A vertex $v_k \in V$ reachable from vertex $v_i \in V$ if there is a path from v_i to v_k . A vertex is globally reachable if it can be reached from every vertex in $\mathcal{G}(V, E)$. The graph is said to be strongly connected, if all vertices of $\mathcal{G}(V, E)$ are globally reachable.

III. THE CONTROL SYSTEM

This section presents the controllers used to achieve the control goals of Section II. First the yaw controller is introduced consisting of the LOS guidance law and a feedback controller. Then the surge controller is introduced including the formation control law.

A. Yaw Control

For convergence of each vessel individual to the path, we propose to use the integral LOS guidance law introduced by [11] to control the desired heading angle, defined as:

$$\psi_{ILOS} \triangleq -\tan^{-1}\left(\frac{y+\sigma y_{\text{int}}}{\Delta}\right), \quad \Delta > 0, \quad (9a)$$

$$\dot{y}_{\text{int}} = \frac{\Delta y}{(y+\sigma y_{\text{int}})^2 + \Delta^2}, \quad (9b)$$

with $\sigma > 0$ the integral gain and Δ the look-ahead distance. As shown in [11] the integral of the cross-track error y allows the vessel to keep a nonzero yaw angle when the vehicle is on the desired path. Moreover, when the cross-track error is large, the integral action becomes small due to the definition in (9b), thus reducing the risk of integrator wind-up. To track the desired yaw angle we define $\psi_d \triangleq \psi_{ILOS}$ and apply the following feedback linearising PD controller to (4f):

$$\tau_r = -F_r(u_r, v_r, r) + \ddot{\psi}_d - k_\psi(\psi - \psi_d) - k_r(\dot{\psi} - \dot{\psi}_d), \quad (10)$$

with $k_\psi > 0$ and $k_r > 0$ constant controller gains. This controller assures that ψ and r exponentially track ψ_d and $\dot{\psi}_d$ respectively.

B. Surge control

A second controller is used to make the relative surge speed of each vessel track the surge speed trajectory

$$u_{c_j} = U_{rd} - g\left(\sum_{i \in \mathcal{A}_j} (x_j - x_i - d_{ji})\right), \quad (11)$$

consisting of the desired constant relative surge velocity U_{rd} and $g(x) : \mathbb{R} \rightarrow \mathbb{R}$ should be a continuously differentiable saturation-like function that satisfies

$$\begin{aligned} -a \leq g(x) \leq a, \quad \forall x \in \mathbb{R}, \quad g(0) = 0, \\ 0 < g'(x) \leq \mu, \quad \forall x \in \mathbb{R}, \quad g'(x) \triangleq dg/dx \end{aligned} \quad (12)$$

where a is the parameter from Assumptions 3 and 4, and $\mu > 0$ is an arbitrary constant. This also implies that the function $g(x)$ should be a sector function belonging to the sector $[0, \mu]$. A suitable choice for $g(x)$ is for example

$$g(x) \triangleq \frac{2a}{\pi} \tan^{-1}(x). \quad (13)$$

To make $u_{r_j}(t)$ track u_{c_j} the following feedback linearising P controller is applied to (4d) (omitting the vessel-specific subscript):

$$\tau_u = -F_{u_r}(v_r, r) + \frac{d_{11}}{m_{11}} u_c + \dot{u}_c - k_{u_r}(u_r - u_c), \quad (14)$$

with $k_{u_r} > 0$ a constant gain. As in [13], part of the damping is not cancelled to guarantee some robustness w.r.t. model uncertainties.

Inspired by [11], [13], and [18] we formulate the main theorem of this paper, using the notation $X^{(\cdot)} \triangleq X(\cdot)$ and $Y^{(\cdot)} \triangleq Y(\cdot)$.

Theorem 1: Consider n vessels described by the dynamical system (4). If Assumptions 1-4 hold, and if the communication digraph $\mathcal{G}(V, E)$ has at least one globally reachable vertex, and the look-ahead distance Δ and the integral gain σ satisfy the conditions

$$\Delta > \frac{|X_j^{U_{rd}+a}|}{|Y_j^{U_{rd}-a}|} \left[\frac{5}{4} \frac{U_{rd} + V_{\max} + a + \sigma}{U_{rd} - V_{\max} - a - \sigma} + 1 \right], \quad (15)$$

$$0 < \sigma < U_{rd} - V_{\max} - a, \quad (16)$$

for $j = 1, \dots, n$, then the controllers (9)-(14) guarantee achievement of the control objectives (5)-(8).

IV. PROOF OF THEOREM 1

To prove Theorem 1 we need to consider the closed-loop system consisting of the path-following error dynamics and the formation error dynamics, and show that the origin of this closed-loop system is UGAS. Therefore we first introduce the error system of the path-following dynamics for each vessel. We then consider the along-path dynamics for each vessel to analyse the formation dynamics. Next we formulate the aggregate system for all the vessels and consider the stability of the origin of the closed-loop system.

A. Single Vessel Dynamics

We consider a single vessel in this part and therefore omit the subscript j in the analysis. The dynamical system (4) is considered in closed loop with the controllers (9)-(14).

We introduce the vector $\xi \triangleq [\tilde{u}_r, \tilde{\psi}, \tilde{r}]^T$, with the tracking errors $\tilde{u}_r \triangleq u_r - u_c$, $\tilde{\psi} \triangleq \psi - \psi_d$, and $\tilde{r} \triangleq r - \dot{\psi}_d$. The dynamics of ξ can be found by applying the controllers (10) and (14) to the dynamical system (4) resulting in:

$$\dot{\xi} = \begin{bmatrix} -k_{u_r} - \frac{d_{11}}{m_{11}} & 0 & 0 \\ 0 & 0 & 1 \\ 0 & -k_\psi & -k_r \end{bmatrix} \xi \triangleq \Sigma \xi. \quad (17)$$

The system (17) is linear and time-invariant and k_{u_r} , k_ψ , k_r , and d_{11}/m_{11} are strictly positive. Consequently, Σ is Hurwitz and the origin of (17) is uniformly globally exponentially stable (UGES).

To guarantee convergence to the path and path following we turn our attention to the unactuated dynamics of the cross-track variable (4b) and the relative sway velocity (4e) combined with the guidance law (9). The dynamics of the $y - v_r$ subsystem is given by:

$$\dot{y}_{\text{int}} = \frac{\Delta y}{(y+\sigma y_{\text{int}})^2 + \Delta^2} \quad (18)$$

$$\dot{y} = (\tilde{u}_r + u_c) \sin(\tilde{\psi} + \psi_d) + v_r \cos(\tilde{\psi} + \psi_d) + V_y \quad (19)$$

$$\dot{v}_r = X(\tilde{u}_r + u_c)(\dot{\tilde{\psi}} + \dot{\psi}_d) + Y(\tilde{u}_r + u_c)v_r. \quad (20)$$

The equilibrium of the $y - v_r$ systems for $u_c = U_{rd}$ satisfies:

$$y_{\text{int}}^{\text{eq}} = \frac{\Delta}{\sigma} \frac{V_y}{\sqrt{U_{rd}^2 - V_y^2}}, \quad y^{\text{eq}} = D_j, \quad v_r^{\text{eq}} = 0. \quad (21)$$

The equilibrium is moved to the origin by defining $e_1 \triangleq y_{\text{int}} - y_{\text{int}}^{\text{eq}}$ and $e_2 \triangleq (y - D_j) + \sigma e_1$. Substituting (9a) for ψ_d and factorizing the result w.r.t. ξ leads to the interconnected dynamics

$$[\dot{e}_1, \dot{e}_2, \dot{v}_r]^T = \mathbf{A}[e_1, e_2, v_r]^T + \mathbf{B}f(e_2) + \mathbf{C}g(x) - \mathbf{H}\xi \quad (22a)$$

$$\dot{\xi} = \Sigma \xi. \quad (22b)$$

with \mathbf{A} as in (23) and \mathbf{B} , \mathbf{C} , and \mathbf{H} defined as:

$$\mathbf{B}(e_2) \triangleq \begin{bmatrix} 0 & V_y & -\frac{\Delta X^{u_c} V_y}{(e_2 + \sigma y_{\text{int}}^{\text{eq}})^2 + \Delta^2} \end{bmatrix}^T, \quad (24)$$

$$\mathbf{C}(e_2) \triangleq \begin{bmatrix} 0 & \frac{\sigma y_{\text{int}}^{\text{eq}}}{(e_2 + \sigma y_{\text{int}}^{\text{eq}})^2 + \Delta^2} & \frac{\Delta X^{u_c} \sigma y_{\text{int}}^{\text{eq}}}{((e_2 + \sigma y_{\text{int}}^{\text{eq}})^2 + \Delta^2)^{3/2}} \end{bmatrix}^T, \quad (25)$$

$$\mathbf{H}(y, y_{\text{int}}, \psi_d, v_r, \xi) \triangleq \begin{bmatrix} 0 & 0 \\ -\frac{\Delta X(\tilde{u}_r + u_c)}{(e_2 + \sigma y_{\text{int}}^{\text{eq}})^2 + \Delta^2} & 1 \end{bmatrix} \begin{bmatrix} h_y^T \\ h_{v_r}^T \end{bmatrix}, \quad (26)$$

$$\mathbf{A}(e_2) \triangleq \begin{bmatrix} -\frac{\sigma\Delta}{(e_2+\sigma y_{\text{int}}^{\text{eq}})^2+\Delta^2} & \frac{\Delta}{(e_2+\sigma y_{\text{int}}^{\text{eq}})^2+\Delta^2} & 0 \\ -\frac{\sigma^2\Delta}{(e_2+\sigma y_{\text{int}}^{\text{eq}})^2+\Delta^2} & \left(\frac{\sigma\Delta}{(e_2+\sigma y_{\text{int}}^{\text{eq}})^2+\Delta^2} - \frac{u_c}{\sqrt{(e_2+\sigma y_{\text{int}}^{\text{eq}})^2+\Delta^2}} \right) & \frac{\Delta}{\sqrt{(e_2+\sigma y_{\text{int}}^{\text{eq}})^2+\Delta^2}} \\ \frac{\sigma^2\Delta^2 X^{u_c}}{((e_2+\sigma y_{\text{int}}^{\text{eq}})^2+\Delta^2)^2} & \left(\frac{u_c\Delta X^{u_c}}{((e_2+\sigma y_{\text{int}}^{\text{eq}})^2+\Delta^2)^{3/2}} - \frac{\sigma\Delta^2 X^{u_c}}{((e_2+\sigma y_{\text{int}}^{\text{eq}})^2+\Delta^2)^2} \right) & \left(Y^{u_c} - \frac{\Delta^2 X^{u_c}}{((e_2+\sigma y_{\text{int}}^{\text{eq}})^2+\Delta^2)^{3/2}} \right) \end{bmatrix} \quad (23)$$

with \mathbf{h}_y^T and $\mathbf{h}_{v_r}^T$ defined in Appendix I and

$$f(e_2) = 1 - \frac{\sqrt{(\sigma y_{\text{int}}^{\text{eq}})^2 + \Delta^2}}{\sqrt{(e_2 + \sigma y_{\text{int}}^{\text{eq}})^2 + \Delta^2}}. \quad (27)$$

Note that $f(e_2)$ satisfies the following bound:

$$|f(e_2)| \leq \frac{|e_2|}{\sqrt{(e_2 + \sigma y_{\text{int}}^{\text{eq}})^2 + \Delta^2}} \quad (28)$$

and that $\mathbf{H}\boldsymbol{\xi}$ contains the terms vanishing at $\boldsymbol{\xi} = \mathbf{0}$.

B. Formation Dynamics

To analyse the formation dynamics we use the along-path dynamics of the vessels. The proof follows along the lines of that in [18], but with relative velocities and the inclusion of the adaptation that comes from the integral effect in the guidance law, which leads to new couplings. Since the path is aligned with the x -axis of the inertial frame, the along-path dynamics for each vessel is given by:

$$\dot{x} = u_r \cos(\psi) - v_r \sin(\psi) + V_x. \quad (29)$$

Using the expressions $u_r = \tilde{u}_r + u_c$, $\psi = \tilde{\psi} + \psi_d$, and $u_c = U_{rd} - g(x)$, with $g(x)$ defined as in (12), (29) can be rewritten as

$$\dot{x} = U_{rd} \cos(\psi) - g(x) \cos(\psi_d) + V_x + \mathbf{h}^T(\boldsymbol{\zeta}, x)\boldsymbol{\zeta}, \quad (30)$$

where $\boldsymbol{\zeta} \triangleq [\boldsymbol{\xi}^T, e_1, e_2, v_r]^T$ and $\mathbf{h}^T\boldsymbol{\zeta}$ contains the terms vanishing at $\boldsymbol{\zeta} = \mathbf{0}$. Furthermore, we can split $\psi_d = \psi_{ss} + \psi_t$ where ψ_{ss} is the steady-state path-following angle (see Fig. 1) and ψ_t a transient part that disappears when $e_2 = 0$ resulting in

$$\dot{x} = U_{rd} \cos(\psi) - g(x) \cos(\psi_{ss}) + V_x + \mathbf{h}_x^T(\boldsymbol{\zeta}, x)\boldsymbol{\zeta}. \quad (31)$$

Consequently, $\mathbf{h}_x^T \triangleq [h_{x,1}, \dots, h_{x,6}]^T$ is given by

$$\begin{aligned} h_{x,1} &= \cos(\tilde{\psi} + \psi_d) \\ h_{x,2} &= g(x) \left[\frac{\sin(\tilde{\psi})}{\tilde{\psi}} \sin(\psi_d) - \frac{\cos(\tilde{\psi})-1}{\tilde{\psi}} \cos(\psi_d) \right] \\ h_{x,5} &= g(x) \left[\frac{\sin(\psi_t)}{e_2} \sin(\psi_{ss}) - \frac{\cos(\psi_t)-1}{e_2} \cos(\psi_{ss}) \right] \\ h_{x,3} &= h_{x,4} = 0; \quad h_{x,6} = \sin(\tilde{\psi} + \psi_d) \end{aligned} \quad (32)$$

where $h_{x,5}$ is related to ψ_t and disappears when $e_2 = 0$.

We now use that U_{rd} can be expressed in terms of the desired velocity $u_x(t)$ in the inertial frame, the component of the ocean current along the path V_x , and the angle ψ . From the geometry of the problem (see Fig. 2) it can be verified that the following holds

$$U_{rd} \cos(\psi) = u_x(t) - V_x. \quad (33)$$

If we substitute (33) in (31) we obtain:

$$\dot{x} = u_x(t) - g(x) \cos(\psi_{ss}) + \mathbf{h}_x^T(\boldsymbol{\zeta}, x)\boldsymbol{\zeta}. \quad (34)$$

More specifically, for the formation we can write (34) as

$$\dot{x}_j = u_x(t) - g \left(\sum_{i \in A_j} (x_j - x_i - d_{ji}) \right) \cos(\psi_{ss_j}) + \mathbf{h}_{x_j}^T \boldsymbol{\zeta}_j \quad (35)$$

with $j = 1, \dots, n$. As in [18] a change of coordinates can be done where $\theta_j \triangleq x_j - d_j - \int_{t_0}^t u_x(s) ds$ for $j = 1, \dots, n$ where d_j is such that $d_j - d_i = d_{ji}$, for $j, i = 1, \dots, n$. This results in

$$\dot{\theta}_j = -g \left(\sum_{i \in A_j} (\theta_j - \theta_i) \right) \cos(\psi_{ss_j}) + \mathbf{h}_{x_j}^T(\boldsymbol{\zeta}_j, \boldsymbol{\theta})\boldsymbol{\zeta}_j, \quad (36)$$

for $j = 1, \dots, n$. It can be verified that $\theta_j - \theta_i = 0 \forall i, j = 1, \dots, n$ implies that (8) is achieved. Moreover, since \tilde{u}_{r_j} converges exponentially to zero and $u_{r_j} = \tilde{u}_{r_j} + u_{c_j}$, exponential convergence in (8) implies exponential convergence in (7). Hence, it suffices to analyse (36) to prove achievement of both (7) and (8).

We now write the system in vector form by defining the aggregate state $\boldsymbol{\theta} \triangleq [\theta_1, \dots, \theta_n]^T$, the aggregate function $\mathbf{g}(\mathbf{x}) \triangleq [g(x_1), \dots, g(x_n)]^T$, and the aggregate matrices $\mathbf{\Lambda} \triangleq [\text{diag}\{\cos(\psi_{ss_1}), \dots, \cos(\psi_{ss_n})\}]$, $\boldsymbol{\zeta} \triangleq [\boldsymbol{\zeta}_1^T, \dots, \boldsymbol{\zeta}_n^T]^T$, and $\mathbf{H}_x \triangleq [\mathbf{h}_{x_1}, \dots, \mathbf{h}_{x_n}]^T$. Such that (36) can be written as

$$\dot{\boldsymbol{\theta}} = -\mathbf{\Lambda}\mathbf{g}(\mathbf{L}\boldsymbol{\theta}) + \mathbf{H}_x(\boldsymbol{\zeta}, \boldsymbol{\theta})\boldsymbol{\zeta} \quad (37)$$

where the \mathbf{L} is the Laplacian matrix of the graph \mathcal{G} with elements:

$$l_{ji} \triangleq \begin{cases} \delta_j & \text{if } j = i \\ -1, & \text{if } j \neq i \wedge (j, i) \in E, j, i = 1, \dots, n \\ 0, & \text{otherwise} \end{cases} \quad (38)$$

with δ_j the number of outgoing edges from v_j . By definition the Laplacian has one or more eigenvalues at zero with the vector of all ones as eigenvector. If the graph is strongly connected -i.e. it has n globally reachable vertices- then the zero eigenvalue is simple and \mathbf{L} is symmetric and positive semi-definite (see [28], [29]).

Remark 4: Although the system equation has differences, the structure (37) is equivalent to the system considered in [18] except for the multiplication with the matrix $\mathbf{\Lambda}$.

As stated in [18] the consensus properties of the along-path dynamics cannot be determined by simply analysing its stability properties, since it can have multiple equilibria depending on the network topology. Therefore, a coordinate transform is proposed in [18, Lemma 2] which can also be derived for system equation (38).

Lemma 1 ([18, Lemma 2]): Consider system (37). Under the conditions of Theorem 1, there exists a coordinate transformation $\boldsymbol{\phi} \triangleq \mathbf{T}\boldsymbol{\theta}$, $\mathbf{T} \in \mathbb{R}^{(n-1) \times n}$, such that the following holds:

- 1) $\boldsymbol{\phi} = \mathbf{0}$ implies that $\theta_1 = \dots = \theta_n$;
- 2) the dynamics of $\boldsymbol{\phi}$ are of the form

$$\dot{\boldsymbol{\phi}} = \mathbf{f}(\boldsymbol{\phi}) + \mathbf{G}(\boldsymbol{\zeta}, \boldsymbol{\phi})\boldsymbol{\zeta} \quad (39)$$

with $\mathbf{G}(\boldsymbol{\zeta}, \boldsymbol{\phi})$ globally bounded, uniformly in $\boldsymbol{\zeta}$ and $\boldsymbol{\phi}$;

- 3) $\dot{\boldsymbol{\phi}} = \mathbf{f}(\boldsymbol{\phi})$ is UGAS with positive definite and radially unbounded Lyapunov function $V = V(\boldsymbol{\phi})$ satisfying

$$\frac{\partial V}{\partial \boldsymbol{\phi}}(\boldsymbol{\phi})\mathbf{f}(\boldsymbol{\phi}) \leq -W(\boldsymbol{\phi}) < 0, \quad \forall \boldsymbol{\phi} \in \mathbb{R}^{n-1} \setminus \{\mathbf{0}\} \quad (40)$$

$$\left\| \frac{\partial V}{\partial \boldsymbol{\phi}}(\boldsymbol{\phi}) \right\| \leq C_1, \quad \forall \boldsymbol{\phi} \in \mathbb{R}^{n-1}. \quad (41)$$

Proof: The proof of Lemma 1 is given in Appendix II. ■

C. The closed-loop system

We can now write the closed-loop system as:

$$\dot{\boldsymbol{\phi}} = \mathbf{f}(\boldsymbol{\phi}) + \mathbf{G}(\boldsymbol{\zeta}, \boldsymbol{\phi})\boldsymbol{\zeta} \quad (42a)$$

$$[\dot{e}_1, \dot{e}_2, \dot{v}_r]^T = \mathbf{A}[e_1, e_2, v_r]^T + \mathbf{B}f(e_2) + \mathbf{C}g(x) - \mathbf{H}\boldsymbol{\xi} \quad (42b)$$

$$\dot{\boldsymbol{\xi}} = \boldsymbol{\Sigma}\boldsymbol{\xi}. \quad (42c)$$

Remark 5: Note that by a slight abuse of notation (42b) contains $g(x)$ instead of $g(\phi)$ and that the cross-track error system is in a non-aggregate form. This is done to make the analysis more clear, since path following is considered for individual vessels, while the along-path dynamics (42a) considers multiple vessels.

Remark 6: Note that (42b) contains a term depending on $g(x)$, hence (42) is a feedback-interconnected system and not a cascaded system. Consequently, we cannot use classical cascaded systems theory to prove stability of the path following problem as is done in [13] and for the formation path following problem as in [18].

Remark 7: Note that the term $Cg(x)$ is a result of the combination of integral action/adaptation. Having only one of these features, as in [13] and [18], this term would be zero. Therefore the feedback-interconnection structure is a result of the combination of integral effect/adaptation together with the formation keeping scheme.

Therefore, we propose to use a technique to grow from a feedback to a cascade-interconnected system by ‘breaking the loop’, as introduced in [26]. In [26] it is shown how a system of the form:

$$\dot{x}_1 = f_1(t, x_1) + g(t, x_1, x_2) \quad (43a)$$

$$\dot{x}_2 = f_2(t, x_1, x_2) \quad (43b)$$

can be analysed as a cascaded system of the form

$$\dot{\xi}_1 = f_1(t, \xi_1) + g(t, \xi_1, \xi_2)\xi_2 \quad (44a)$$

$$\dot{\xi}_2 = f_2(t, x_1(t), \xi_2) = \tilde{f}_2(t, \xi_2) \quad (44b)$$

where $f_2(t, x_1(t), \xi_2)$ depends on the *parameter* x_1 , with $x_1(t)$ denoting solutions of (43a).

In [26] three cases are identified for the order of functions f_1 and g w.r.t. x_1 , for each fixed x_2 . In this case f_1 is given by (34), which is the nominal path-following dynamics with $x_1 = x$ for an individual vessel, and g is given by (32), which is the perturbing term of the path-following dynamics with $x_2 = \zeta$. Comparing (34) and (32) it can be seen that in the case considered here the functions are of the same order w.r.t. $g(x)$. To prove UGAS when the functions f_1 and g are of the same order w.r.t. x_1 the following conditions are given [26]:

- 1) $x_1 = 0$ is a UGAS equilibrium for $\dot{x}_1 = f_1(t, x_1)$.
- 2) The solutions of (43) are uniformly globally bounded.

Proposition 1 ([26, Proposition 2]): Under Condition 1 and the conditions of Theorem 2 the origin of (42) is UGAS.

Proof: For the case considered here condition 1) translates to the closed-loop system satisfying the following condition:

Condition 1: $\phi = 0$ is a UGAS equilibrium for $\dot{\phi} = \mathbf{f}(\phi)$.

Condition 1 is verified by the proof of claim 3) from Lemma 1.

We then use [26, Theorem 2] which gives sufficient conditions for Condition 2 to be satisfied. The first condition to be verified is

Condition 2a: There exists a C^1 positive definite radially unbounded function $\tilde{V} : \mathbb{R} \times \mathbb{R}^{n_1} \rightarrow \mathbb{R}_{\geq 0}$, $\alpha_1 \in \mathcal{K}_\infty$ and continuous non-decreasing functions $\alpha_4, \alpha'_4 : \mathbb{R}_{\geq 0} \times \mathbb{R} \rightarrow \mathbb{R}_{\geq 0}$ such that

$$\tilde{V}(t, x_1) \geq \alpha_1(|x_1|) \quad (45)$$

and that,

$$\dot{\tilde{V}}_{(42a)}(t, x_1) \leq \alpha_4(|x_1|)\alpha'_4(|x_2|); \quad (46)$$

$$\int_a^\infty \frac{d\tilde{v}}{\alpha_4(\alpha_1^{-1}(\tilde{v}))} = \infty \quad (47)$$

Condition 2a can be verified using the function

$$\tilde{V}_{(42a)}(\phi) = \frac{1}{2}\phi^2 \quad (48)$$

which is clearly \mathcal{K}_∞ , satisfying (45). From (48) it follows that

$$\dot{\tilde{V}}_{(42a)}(\phi) \triangleq \frac{\partial \tilde{V}}{\partial t} + \frac{\partial \tilde{V}}{\partial \phi} [\mathbf{f}(\phi) + \mathbf{G}(\zeta, \phi)\zeta] = \phi \dot{\phi}. \quad (49)$$

Using (77) and (32) it can be verified that functions

$$\alpha_4(|\phi|) \triangleq |\phi| \quad (50)$$

$$\alpha'_4(|\zeta|) \triangleq \begin{bmatrix} -L_1 - L_2 \\ -M_3^T \end{bmatrix} \cdot [1 + |\tilde{u}_r| + 8a|\tilde{\psi}| + |v_r|] \quad (51)$$

satisfy the inequality

$$\dot{\tilde{V}}_{(42a)}(\phi) \leq \alpha_4(|\phi|)\alpha'_4(|\zeta|)$$

with $\alpha_4, \alpha'_4 : \mathbb{R}_{\geq 0} \times \mathbb{R} \rightarrow \mathbb{R}_{\geq 0}$ continuous and non-decreasing w.r.t. their arguments.

To verify that (47) holds, note that $\alpha_1^{-1}(\tilde{v}) = \sqrt{2\tilde{v}}$ and consequently it holds that

$$\int_a^\infty \frac{d\tilde{v}}{\alpha_4(\alpha_1^{-1}(\tilde{v}))} = \int_a^\infty \frac{d\tilde{v}}{\sqrt{2\tilde{v}}} = \infty.$$

Condition 2b: We dispose of a C^1 function $V : \mathbb{R} \times \mathbb{R}^{n_1} \rightarrow \mathbb{R}_{\geq 0}$, $\alpha_1, \alpha_2 \in \mathcal{K}_\infty$, and a positive semidefinite function W such that

$$\alpha_1(|x_1|) \leq V(t, x_1) \leq \alpha_2(|x_1|) \quad (52)$$

$$\frac{\partial V}{\partial t} + \frac{\partial V}{\partial x_1} f_1(t, x_1) \leq -W(x_1) \quad (53)$$

for all $t \in [t_o, t_{\max})$ and all $x_1 \in \mathbb{R}^{n_1}$.

Condition 2b holds as a direct consequence of Condition 1 being satisfied.

Condition 2c: There exists $\beta \in \mathcal{KL}$ such that the solutions $x_2(t, t_o, x_{2o}, x_1)$ of $\dot{x}_2 = \tilde{f}_2(t, x_2)$ satisfy

$$|x_2(t, t_o, x_{2o}, x_1)| \leq \beta(|x_{2o}|, t - t_o) \quad \forall t \in [t_o, t_{\max}). \quad (54)$$

Condition 2c can be verified by showing boundedness of the solutions of (42b).

Remark 8: Formally boundedness of the solutions of (42b-42c) should be shown. However, since (42c) is a linear GES system, cascaded systems theory [30] gives that boundedness of the solutions of (42b) can be analysed without the perturbing term, since this is bounded in its arguments, and implies boundedness of the solutions of (42b-42c).

Neglecting the perturbing dynamics $\mathbf{H}(y, y_{\text{int}}, \psi_d, v_r, \xi)\xi$, we propose the same Lyapunov function candidate as in [13]:

$$V \triangleq \frac{1}{2}\sigma^2 e_1^2 + \frac{1}{2}e_2^2 + \frac{1}{2}\mu v_r^2. \quad (55)$$

Taking the time-derivative of this Lyapunov function along the solutions of (42b), omitting $\mathbf{H}\xi$, results in

$$\begin{aligned} \dot{V} \leq & -W_1(|\bar{e}_1|, |v_r|) - W_2(|\bar{e}_2|, |v_r|) + a\sigma y_{\text{int}}^{\text{eq}}|\bar{e}_2| \\ & + a\mu \frac{\Delta |X^{uc}| \sigma y_{\text{int}}^{\text{eq}}}{((e_2 + \sigma y_{\text{int}}^{\text{eq}})^2 + \Delta^2)^{3/2}} |v_r| \end{aligned} \quad (56)$$

with $\bar{e}_i \triangleq e_i / \sqrt{(e_2 + \sigma y_{\text{int}}^{\text{eq}})^2 + \Delta^2}$ for $i = 1, 2$, and where

$$\begin{aligned} W_1 \triangleq & \sigma^3 \Delta |\bar{e}_1|^2 - \mu \sigma^2 \frac{|X^{uc}|}{\Delta} |\bar{e}_1| |v_r| + \mu \eta \left(|Y^{uc}| - \frac{|X^{uc}|}{\Delta} \right) |v_r|^2 \\ \triangleq & \mathbf{w}_1^T \mathbf{P}_1 \mathbf{w}_1 \end{aligned} \quad (57)$$

$$W_2 \triangleq \Delta [|\bar{e}_2| |v_r|] \begin{bmatrix} \beta & -\alpha \\ -\alpha & \alpha(2\alpha - 1) \end{bmatrix} \begin{bmatrix} |\bar{e}_2| \\ |v_r| \end{bmatrix} \triangleq \mathbf{w}_2^T \mathbf{P}_2 \mathbf{w}_2 \quad (58)$$

with $0 < \eta < 1$, $\beta \triangleq U_{rd} - a - V_{\max} - \sigma$ and α is given by:

$$\alpha \triangleq (1 - \eta) \frac{(U_{rd} - a - V_{\max} - \sigma)(\Delta |Y^{uc}| - |X^{uc}|)}{|X^{uc}|(U_{rd} + a + V_{\max} + \sigma)}. \quad (59)$$

Notice that (56) has a term that is linear in $|\bar{e}_2|$ and a term that is linear in $|v_r|$. The linear terms do not appear in [13], since

they are induced by the formation control influencing the velocity. The linear terms make it impossible to prove UGAS and ULES with the Lyapunov function candidate (55) as in [13]. However, we propose to dominate the linear terms using the quadratic term in $|\bar{e}_2|$ from W_2 and the quadratic term $|v_r|$ in W_1 . Consequently showing boundedness of the solutions and hence satisfying Condition 2c.

Part 1: Dominating $a\sigma y_{\text{int}}^{\text{eq}}|\bar{e}_2|$: The term $\Delta\beta|\bar{e}_2|^2$ from W_2 can be used to dominate $a\sigma y_{\text{int}}^{\text{eq}}|\bar{e}_2|$. Consider the inequality

$$a\sigma y_{\text{int}}^{\text{eq}}|\bar{e}_2| - \Delta\beta|\bar{e}_2|^2 \leq \Delta(U_{rd} - a - V_{\text{max}} - \sigma)|\bar{e}_2|^2 - \Delta V_{\text{max}}|\bar{e}_2|$$

The quadratic term will dominate the linear term if $U_{rd} > 2V_{\text{max}} + a$ and $|\bar{e}_2| > 1$. Since W_2 is positive definite W_2 will dominate the linear term in $|\bar{e}_2|$ for sufficiently large values of $|\bar{e}_2|$ and an appropriate choice of β and α .

Remark 9: The bound on U_{rd} is more conservative than the bound given in [13]. This can be explained by the need of additional freedom to change the surge velocity for formation keeping.

Part 2: Dominating $\frac{a\mu\Delta|X^{uc}||\sigma y_{\text{int}}^{\text{eq}}}{((e_2 + \sigma y_{\text{int}}^{\text{eq}})^2 + \Delta^2)^{3/2}}|v_r|$: To dominate this term we use the quadratic term from W_1 and consider the inequality

$$\begin{aligned} & \frac{a\mu\Delta|X^{uc}||\sigma y_{\text{int}}^{\text{eq}}}{((e_2 + \sigma y_{\text{int}}^{\text{eq}})^2 + \Delta^2)^{3/2}}|v_r| - \mu\eta \left(|Y^{uc}| - \frac{|X^{uc}|}{\Delta} \right) |v_r|^2 \\ & \leq \mu \frac{|X^{uc}|}{2\Delta} V_{\text{max}} |v_r| - \mu\eta \left(|Y^{uc}| - \frac{|X^{uc}|}{\Delta} \right) |v_r|^2. \end{aligned} \quad (60)$$

Using (60) it can be verified that the quadratic term dominates the linear term if

$$\Delta > \frac{|X^{uc}|}{|Y^{uc}|} \left[\frac{V_{\text{max}}}{2\eta} + 1 \right]. \quad (61)$$

According to [13] positive definiteness of W_1 is guaranteed if $1/5 \leq \eta < 1$. Hence, the linear term is dominated by the quadratic term whilst positive definiteness of W_1 is guaranteed if η satisfies $1/5 \leq \eta < 1$, Δ satisfies (61), and $|v_r|$ is sufficiently large.

Negative definiteness of \dot{V} : Now denoting the minimum eigenvalues of positive definite matrices \mathbf{P}_1 and \mathbf{P}_2 from (56) by $\lambda_{\min}(\mathbf{P}_1)$ and $\lambda_{\min}(\mathbf{P}_2)$ respectively and taking into account the bounds derived in the preceding, we can rewrite (56) as

$$\begin{aligned} \dot{V} & \leq -\lambda_{\min}(\mathbf{P}_1)\|\mathbf{w}_1\|^2 - \lambda_{\min}(\mathbf{P}_2)\|\mathbf{w}_2\|^2 \\ & \quad + \mu|X^{uc}|/(2\Delta)V_{\text{max}}\|\mathbf{w}_1\| + \Delta V_{\text{max}}\|\mathbf{w}_2\|. \end{aligned} \quad (62)$$

From (62) it can be seen that for large values of $|\bar{e}_2|$ and $|v_r|$, and consequently \mathbf{w}_1 and \mathbf{w}_2 , \dot{V} will become negative definite. Hence, the solutions $|\zeta(t, t_o, z_o, x)|$ of $\dot{\zeta} = \tilde{f}_2(t, \zeta_2)$ are bounded from above and below and satisfy Condition 2c.

Condition 2 can now be verified according to [26, Theorem 2]:

Theorem 2 ([26, Theorem 2]): Consider system (42) under the following conditions:

- 1) Condition 2a, 2b, and 2c hold;
- 2) there exist $\alpha_5, \alpha'_5 \in \mathcal{K}$ such that

$$\|[L_g V]\| \leq \alpha_5(|x_1|)\alpha'_5(|x_2|) \quad (63)$$

and for each $r > 0$ there exist $\lambda_r, \eta_r > 0$ such that

$$t \geq 0, |x_1| \geq \eta_r \implies \alpha_5(|x_1|) \leq \lambda_r W(x_1) \quad (64)$$

Then, the solutions of (42) are uniformly globally bounded.

The first condition of Theorem 2 has already been shown to hold true by verification of the conditions. It can be verified that the second condition holds with:

$$\alpha_5(|\phi|) \triangleq [p_m a \|g(\phi_1)\| \quad \delta \|\phi_2\|]^T \quad (65)$$

$$\alpha'_5(|\zeta|) \triangleq \alpha'_4(|\zeta|). \quad (66)$$

Consequently, Theorem 2 holds and the solutions of (42) are globally bounded.

It is shown that both Condition 1 and Theorem 2 hold and hence Proposition 1 holds and the origin of (42) is UGAS. ■

That the origin of (42) is UGAS implies that the control goals (5)-(8) are achieved. This concludes the proof of Theorem 1.

V. CASE STUDY

In this case study we consider three vessels described by the ship model from [31]. The three vessels each have to follow their specified path \mathcal{P}_i , whilst being affected by a current with an intensity $|V_c| = \sqrt{2}$ [m/s]. The components of the current are chosen as $V_x = -1.1028$ [m/s] and $V_y = 0.8854$ [m/s]. The integral gain for the ILOS guidance law is chosen as $\sigma = 1.5$ [m/s] and the look-ahead distance is chosen to be $\Delta = 200$ [m], which satisfies conditions (15-16) for the given vessels. The gains for the feedback linearising controllers are chosen as $k_{u_r} = 0.1$, $k_{\psi} = 0.04$, and $k_r = 0.9$, following the tuning of the path following controller in [13]. All initial velocities are set to zero and the initial positions and angles (in degrees) are chosen as

$$\begin{bmatrix} x_{1o} \\ y_{1o} \\ \psi_{1o} \end{bmatrix} = \begin{bmatrix} 0 \\ -1000 \\ 180 \end{bmatrix}, \begin{bmatrix} x_{2o} \\ y_{2o} \\ \psi_{2o} \end{bmatrix} = \begin{bmatrix} 0 \\ 500 \\ 90 \end{bmatrix}, \begin{bmatrix} x_{3o} \\ y_{3o} \\ \psi_{3o} \end{bmatrix} = \begin{bmatrix} 0 \\ -500 \\ -90 \end{bmatrix}.$$

The desired relative surge velocity is chosen to be $U_{rd} = 5$ [m/s] and the velocity adaptation parameter as $a = 0.5$ [m/s] to have sufficient freedom to adapt the velocity. Ship 1 can communicate its position to ship 2 and 3, while only ship 3 can communicate its position to ship 1. The path following distances for the formation are $d_{12} = 200$ [m], $d_{13} = 100$ [m], $D_2 = -200$ [m], and $D_3 = 200$ [m]. In Fig. 3 it can be seen that the ships converge to their specified paths and attain the desired formation. We also see how the ships side-slip in order to keep the desired path despite the ocean current acting in the transverse direction of the path. In Fig. 4 the relative surge velocity over time can be seen. We can see that at first ship 1 is at maximal speed while ship 2 and 3 wait until they are at the desired distance by slowing down. After about 340 [s] ship 2 is at the desired position w.r.t. ship 1 and matches its velocity to ship 1. After about 540 [s] the desired formation is achieved and the velocities all converge to the desired surge velocity. The along-path formation errors can be seen in Fig. 5, from which it can be observed that the formation errors converge to zero.

Remark 10: Collision avoidance is not taken into consideration during this case study, which is intended to illustrate the combined path-following and formation control strategy.

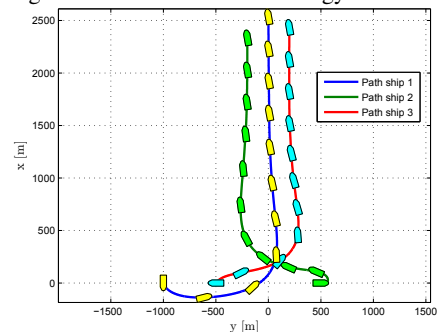


Fig. 3. The paths of the vessels attaining formation.

VI. CONCLUSIONS

In this paper, the problem of path following for formations of underactuated surface vessels under the influence of constant ocean currents is considered. It is shown that n underactuated surface vessels can be controlled to follow a straight-line path whilst

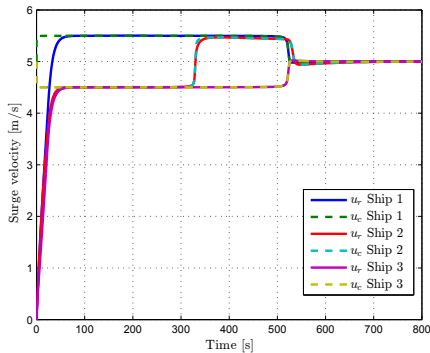


Fig. 4. The relative surge velocities u_r and their desired values u_c .

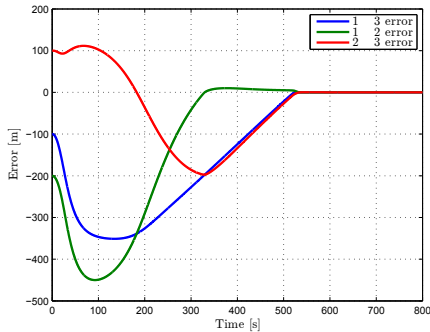


Fig. 5. The along-path formation keeping error between the vehicles.

attaining and maintaining a desired formation. This is achieved by making each vehicle converge to a desired path individually using a ILOS-based cross-track controller, combined with a formation keeping control scheme controlling the along-path position of the vessels using only locally available information. The closed-loop system of the path following and formation control strategy is analysed using theory for nonlinear cascaded systems. This is done by showing that the system, which is feedback interconnected, can be analysed as a cascaded system under certain conditions. Simulation results are presented to validate the theory.

REFERENCES

- [1] F. A. Papoulias, "Bifurcation analysis of line of sight vehicle guidance using sliding modes," *Int. Journal of Bifurcation and Chaos*, vol. 1, no. 4, pp. 849–865, 1991.
- [2] K. Y. Pettersen and E. Lefeber, "Way-point tracking control of ships," in *Proc. of the 40th IEEE Conference on Decision and Control*, 2001, pp. 940–945.
- [3] T. I. Fossen, M. Breivik, and R. Skjetne, "Line-of-sight path following of underactuated marine craft," in *Proc. of the 6th IFAC Conference on Manoeuvring and Control of Marine Craft*, 2003, pp. 244–249.
- [4] E. Fredriksen and K. Y. Pettersen, "Global κ -exponential way-point maneuvering of ships: Theory and experiments," *Automatica*, vol. 42, no. 4, pp. 677–687, 2006.
- [5] E. Peymani and T. I. Fossen, "Speed-varying path following for underactuated marine craft," in *Proc. of the 9th IFAC Conference on Control Applications in Marine Systems*, 2013.
- [6] K. D. Do, Z.-P. Jiang, and J. Pan, "Robust adaptive path following of underactuated ships," *Automatica*, vol. 40, no. 6, pp. 929–944, 2004.
- [7] A. P. Aguiar and J. P. Hespanha, "Trajectory-tracking and path-following of underactuated autonomous vehicles with parametric modeling uncertainty," *IEEE Transactions on Automatic Control*, vol. 52, no. 8, pp. 1362–1379, 2007.
- [8] M. Aicardi, G. Casalino, G. Indiveri, A. Aguiar, P. Encarnação, and A. Pascoal, "A planar path following controller for underactuated marine vehicles," in *Proc. 9th Mediterranean Conference on Control and Automation*, 2001.
- [9] L. Lapiere, D. Soetanto, and A. Pascoal, "Nonlinear path following with applications to the control of autonomous underwater vehicles," in *Proc. of the 42nd IEEE Conference on Decision and Control*, vol. 2, 2003, pp. 1256–1261.

- [10] A. P. Aguiar and A. M. Pascoal, "Dynamic positioning and way-point tracking of underactuated auvs in the presence of ocean currents," *International Journal of Control*, vol. 80, no. 7, pp. 1092–1108, 2007.
- [11] E. Børhaug, A. Pavlov, and K. Y. Pettersen, "Integral los control for path following of underactuated marine surface vessels in the presence of ocean currents," in *Proc. of the 47th IEEE Conference on Decision and Control*, 2008, pp. 4984–4991.
- [12] W. Caharija, K. Y. Pettersen, J. T. Gravdahl, and E. Børhaug, "Path following of underactuated autonomous underwater vehicles in the presence of ocean currents," in *Proc. of the 51th IEEE Conference on Decision and Control*, 2012, pp. 528–535.
- [13] W. Caharija, M. Candeloro, K. Y. Pettersen, and A. J. Sørensen, "Relative velocity control and integral los for path following of underactuated surface vessels," in *Proc. of the 9th IFAC Conference on Manoeuvring and Control of Marine Craft*, 2012.
- [14] H. Bai, M. Arcak, and J. T. Wen, *Cooperative control design*. Springer, 2011, vol. 89.
- [15] K. Y. Pettersen, J. T. Gravdahl, and H. Nijmeijer, *Group coordination and cooperative control*. Springer Berlin, 2006, vol. 336.
- [16] E. Børhaug, A. Pavlov, and K. Y. Pettersen, "Cross-track formation control of underactuated surface vehicles," in *Proc. of the 45th IEEE Conference on Decision and Control*, 2006, pp. 5955–5961.
- [17] —, "Straight line path following for formations of underactuated underwater vehicles," in *Proc. of the 46th IEEE Conference on Decision and Control*, 2007, pp. 2905–2912.
- [18] E. Børhaug, A. Pavlov, E. Panteley, and K. Y. Pettersen, "Straight line path following for formations of underactuated marine surface vehicles," *IEEE Transactions on Control Systems Technology*, vol. 19, no. 3, pp. 493–506, 2011.
- [19] L. Lapiere, D. Soetanto, and A. Pascoal, "Coordinated motion control of marine robots," in *Proceedings of the 6th IFAC Conference on Manoeuvring and Control of Marine Craft*, 2004.
- [20] R. Ghabcheloo, A. P. Aguiar, A. Pascoal, C. Silvestre, I. Kaminer, and J. Hespanha, "Coordinated path-following control of multiple underactuated autonomous vehicles in the presence of communication failures," in *Proc. of the 45th IEEE Conference on Decision and Control*, 2006, pp. 4345–4350.
- [21] —, "Coordinated path-following in the presence of communication losses and time delays," *SIAM Journal on Control and Optimization*, vol. 48, no. 1, pp. 234–265, 2009.
- [22] J. Almeida, C. Silvestre, and A. Pascoal, "Cooperative control of multiple surface vessels in the presence of ocean currents and parametric model uncertainty," *International Journal of Robust and Nonlinear Control*, vol. 20, no. 14, pp. 1549–1565, 2010.
- [23] I.-A. F. Ihle, J. Jouffroy, and T. I. Fossen, "Formation control of marine surface craft: A lagrangian approach," *IEEE Journal of Oceanic Engineering*, vol. 31, no. 4, pp. 922–934, 2006.
- [24] Z. Peng, D. Wang, Z. Chen, X. Hu, and W. Lan, "Adaptive dynamic surface control for formations of autonomous surface vehicles with uncertain dynamics," *IEEE Transactions on Control Systems Technology*, vol. 21, no. 2, pp. 513–520, 2013.
- [25] M. Burger, A. Pavlov, E. Børhaug, and K. Y. Pettersen, "Straight line path following for formations of underactuated surface vessels under influence of constant ocean currents," in *Proc. of the American Control Conference*, 2009, pp. 3065–3070.
- [26] A. Loria, "From feedback to cascade-interconnected systems: Breaking the loop," in *Proc. of the 47th IEEE Conference on Decision and Control*, 2008, pp. 4109–4114.
- [27] T. I. Fossen, *Handbook of Marine Craft Hydrodynamics and Motion Control*. Wiley, 2011.
- [28] M. Mesbahi and M. Egerstedt, *Graph theoretic methods in multiagent networks*. Princeton University Press, 2010.
- [29] C. Godsil and G. Royle, "Algebraic graph theory," *Ser. Springer Graduate Texts in Mathematics*, vol. 207, 2001.
- [30] A. Loria and E. Panteley, "2 cascaded nonlinear time-varying systems: Analysis and design," in *Advanced topics in control systems theory*. Springer, 2005, pp. 23–64.
- [31] E. Fredriksen and K. Y. Pettersen, "Global κ -exponential way-point maneuvering of ships: Theory and experiments," *Automatica*, vol. 42, no. 4, pp. 677–687, 2006.
- [32] Z. Lin, B. Francis, and M. Maggiore, "Necessary and sufficient graphical conditions for formation control of unicycles," *IEEE Transactions on Automatic Control*, vol. 50, no. 1, pp. 121–127, 2005.

APPENDIX I
FUNCTION DEFINITIONS

The functions F_{u_r} , $X(u_r)$, $Y(u_r)$, and F_r are given by:

$$F_{u_r} \triangleq \frac{1}{m_{11}}(m_{22}v_r + m_{23}r), \quad (67)$$

$$X(u_r) \triangleq \frac{m_{23}^2 - m_{11}m_{33}}{m_{22}m_{33} - m_{23}^2}u_r + \frac{d_{33}m_{23} - d_{23}m_{33}}{m_{22}m_{33} - m_{23}^2}, \quad (68)$$

$$Y(u_r) \triangleq \frac{(m_{22} - m_{11})m_{23}}{m_{22}m_{33} - m_{23}^2}u_r - \frac{d_{22}m_{33} - d_{32}m_{23}}{m_{22}m_{33} - m_{23}^2}, \quad (69)$$

$$F_r(u_r, v_r, r) \triangleq \frac{m_{23}d_{22} - m_{22}(d_{32} + (m_{22} - m_{11})u_r)}{m_{22}m_{33} - m_{23}^2}v_r + \frac{m_{23}(d_{23} + m_{11}u_r) - m_{22}(d_{33} + m_{23}u_r)}{m_{22}m_{33} - m_{23}^2}r. \quad (70)$$

Functions $\mathbf{h}_y \triangleq [h_{y1}, h_{y2}, h_{y3}]^T$ and $\mathbf{h}_{v_r} \triangleq [h_{v_r1}, h_{v_r2}, h_{v_r3}]^T$ are given by:

$$\begin{aligned} h_{y,1} &= \sin(\tilde{\psi} + \psi_d), \quad h_{y,3} = 0, \\ h_{y,2} &= u_c \left[\frac{\sin(\tilde{\psi})}{\tilde{\psi}} \cos(\psi_d) + \frac{\cos(\tilde{\psi}) - 1}{\tilde{\psi}} \sin(\psi_d) \right] \\ &\quad + v_r \left[\frac{\cos(\tilde{\psi}) - 1}{\tilde{\psi}} \cos(\psi_d) - \frac{\sin(\tilde{\psi})}{\tilde{\psi}} \sin(\psi_d) \right], \end{aligned} \quad (71)$$

$$\begin{aligned} h_{v_r,1} &= \frac{X(\tilde{u}_r + u_c) - X^{u_c}}{\tilde{u}_r} \gamma(y_{\text{int}}, y, v_r) + v_r \frac{Y(\tilde{u}_r + u_c) - Y^{u_c}}{\tilde{u}_r}, \\ h_{v_r,2} &= 0, \quad h_{v_r,3} = X(\tilde{u}_r - u_c), \end{aligned} \quad (72)$$

with $\gamma(y_{\text{int}}, y, v_r)$ defined as:

$$\begin{aligned} \gamma(y_{\text{int}}, y, v_r) &\triangleq \frac{\Delta(u_c(y + \sigma y_{\text{int}}^{\text{eq}}) - \Delta v_r)}{((e_2 + \sigma y_{\text{int}}^{\text{eq}})^2 + \Delta^2)^{3/2}} - \frac{\Delta V_y}{(e_2 + \sigma y_{\text{int}}^{\text{eq}})^2 + \Delta^2} \\ &\quad - \frac{\sigma \Delta}{((e_2 + \sigma y_{\text{int}}^{\text{eq}})^2 + \Delta^2)^2} (y - D_j). \end{aligned} \quad (73)$$

APPENDIX II
PROOF OF LEMMA 1

The proof for Lemma 1 follows along the lines of the proof given in [18]. However, we now have to account for the matrix $\mathbf{\Lambda}$ in the dynamics (in addition to the interconnection term $\mathbf{H}_x \boldsymbol{\zeta}$ being different). In Theorem 1 it is assumed that the communication graph \mathcal{G} has at least one globally reachable vertex. Therefore in this proof we assume that \mathcal{G} has $1 \leq r < n$ globally reachable vertices. This allows us, without loss of generality, to partition \mathbf{L} as

$$\mathbf{L} = \begin{bmatrix} \mathbf{L}_1 & \mathbf{L}_2 \\ \mathbf{0} & \mathbf{L}_3 \end{bmatrix} \quad (74)$$

where $\mathbf{L}_1 \in \mathbb{R}^{(n-r) \times (n-r)}$ is anti-Hurwitz, i.e., $-\mathbf{L}_1$ is Hurwitz, and satisfies

$$\mathbf{P}\mathbf{L}_1 + \mathbf{L}_1^T \mathbf{P} = \mathbf{Q}, \quad \mathbf{Q} = \mathbf{Q}^T > 0 \quad (75)$$

for some positive definite diagonal matrix \mathbf{P} [32]. The sub-graph corresponding to $\mathbf{L}_3 \in \mathbb{R}^{r \times r}$, i.e. $\mathcal{G}(\mathbf{L}_3)$, is strongly connected. Hence \mathbf{L}_3 is positive semi-definite, with zero as a simple eigenvalue and a corresponding eigenvector $\mathbf{1}_r = [1, \dots, 1]^T \in \mathbb{R}^r$. Consequently, \mathbf{L}_3 can be decomposed into $\mathbf{L}_3 = \mathbf{M}_3 \mathbf{M}_3^T$, where $\mathbf{M}_3 \in \mathbb{R}^{r \times (r-1)}$ has full column rank. A coordinate transform is then given by

$$\boldsymbol{\phi} \triangleq \begin{bmatrix} \mathbf{L}_1 & \mathbf{L}_2 \\ \mathbf{0} & \mathbf{M}_3^T \end{bmatrix} \boldsymbol{\theta} \triangleq \mathbf{T}\boldsymbol{\theta}. \quad (76)$$

We can now verify the claims of Lemma 1.

Claim 1):

$$\boldsymbol{\phi} = \mathbf{0} \Rightarrow \begin{bmatrix} \mathbf{I} & \mathbf{0} \\ \mathbf{0} & \mathbf{M}_3 \end{bmatrix} \boldsymbol{\phi} = \mathbf{L}\boldsymbol{\theta} = \mathbf{0} \Rightarrow \boldsymbol{\theta} = \alpha \mathbf{1}_n, \quad \alpha \in \mathbb{R}.$$

Consequently, $\boldsymbol{\phi} = \mathbf{0}$ implies that $\theta_j = \theta_i$, $j, i = 1, \dots, n$.

Claim 2): Differentiating (76) w.r.t time we obtain

$$\dot{\boldsymbol{\phi}} = \begin{bmatrix} -\mathbf{L}_1 \mathbf{\Lambda}_1 \mathbf{g}_1(\boldsymbol{\phi}_1) - \mathbf{L}_2 \mathbf{\Lambda}_2 \mathbf{g}_2(\boldsymbol{\kappa}) \\ -\mathbf{M}_3^T \mathbf{\Lambda}_2 \mathbf{g}_2(\boldsymbol{\kappa}) \end{bmatrix} + \mathbf{T}\mathbf{H}_x(\boldsymbol{\zeta}, \boldsymbol{\theta})\boldsymbol{\zeta} \quad (77)$$

$$\triangleq \mathbf{f}(\boldsymbol{\phi}) + \mathbf{G}(\boldsymbol{\zeta}, \boldsymbol{\theta})\boldsymbol{\zeta} \quad (78)$$

where $\boldsymbol{\phi} = [\boldsymbol{\phi}_1^T, \boldsymbol{\phi}_2^T]^T$, with $\boldsymbol{\phi}_1 \in \mathbb{R}^{n-r}$ and $\boldsymbol{\phi}_2 \in \mathbb{R}^r$, and we defined $\boldsymbol{\kappa} \triangleq \mathbf{M}_3 \boldsymbol{\phi}_2$ to simplify notation. Moreover, using (32) it is straightforward to verify that $\mathbf{G}(\boldsymbol{\zeta}, \boldsymbol{\phi}) \triangleq \mathbf{T}\mathbf{H}_x(\boldsymbol{\zeta}, \boldsymbol{\phi})$ is globally bounded in its arguments.

Claim 3): Consider the stability properties of the nominal system

$$\begin{bmatrix} \dot{\boldsymbol{\phi}}_1 \\ \dot{\boldsymbol{\phi}}_2 \end{bmatrix} = \begin{bmatrix} -\mathbf{L}_1 \mathbf{\Lambda}_1 \mathbf{g}_1(\boldsymbol{\phi}_1) - \mathbf{L}_2 \mathbf{\Lambda}_2 \mathbf{g}_2(\boldsymbol{\kappa}) \\ -\mathbf{M}_3^T \mathbf{\Lambda}_2 \mathbf{g}_2(\boldsymbol{\kappa}) \end{bmatrix} = \mathbf{f}(\boldsymbol{\phi}). \quad (79)$$

Remark 11): Note that considering the stability properties of the origin of the nominal dynamics means that we consider the stability properties of (77) when the perturbing dynamics has converged. This implies that the cross-track error has converged, and consequently, the desired yaw angle ψ_d is bounded well away from $\pi/2$ and $-\pi/2$. Hence the elements of diagonal matrices $\mathbf{\Lambda}_1$ and $\mathbf{\Lambda}_2$ are bounded away from zero and will have clearly defined minimum eigenvalues of λ_{m_1} and λ_{m_2} respectively.

To show that the origin of (79) is UGAS we use the Lyapunov function candidate

$$V \triangleq \frac{\delta}{2} \|\boldsymbol{\phi}_2\|^2 + \int_0^{\boldsymbol{\phi}_1} \mathbf{P}\mathbf{\Lambda}_1 \mathbf{g}_1(\mathbf{y}) \cdot d\mathbf{y} \quad (80)$$

where \mathbf{P} is the positive definite diagonal solution of (75) and $\delta > 0$ to be chosen at a later stage. The sector property of g and the fact that \mathbf{P} is a positive definite diagonal matrix assure that V is a positive definite function of $\boldsymbol{\phi}_1$ and $\boldsymbol{\phi}_2$. It is straightforward to verify that V is also radially unbounded. Taking the time-derivative of V along the solutions of (79) gives

$$\begin{aligned} \dot{V} &= -\frac{1}{2} \mathbf{g}_1^T(\boldsymbol{\phi}_1) [\mathbf{\Lambda}_1 \mathbf{P} \mathbf{L}_1 \mathbf{\Lambda}_1 + \mathbf{\Lambda}_1 \mathbf{L}_1^T \mathbf{P} \mathbf{\Lambda}_1] \mathbf{g}_1(\boldsymbol{\phi}_1) \\ &\quad - \delta \boldsymbol{\kappa}^T \mathbf{\Lambda}_2 \mathbf{g}_2(\boldsymbol{\kappa}) - \mathbf{g}_1^T(\boldsymbol{\phi}_1) \mathbf{\Lambda}_1 \mathbf{P} \mathbf{L}_2 \mathbf{\Lambda}_2 \mathbf{g}_2(\boldsymbol{\kappa}) \end{aligned} \quad (81)$$

If we substitute for \mathbf{Q} in (81) and take the norm we obtain

$$\dot{V} \leq c \|\mathbf{g}_1(\boldsymbol{\phi}_1)\| \cdot \|\mathbf{g}_2(\boldsymbol{\kappa})\| - \delta \boldsymbol{\kappa}^T \mathbf{\Lambda}_2 \mathbf{g}_2(\boldsymbol{\kappa}) - \frac{q_m}{2} \|\mathbf{g}_1^T(\boldsymbol{\phi}_1)\|^2$$

with $q_m > 0$ the minimum eigenvalue of $\mathbf{\Lambda}_1 \mathbf{Q} \mathbf{\Lambda}_1$ and $c \geq \|\mathbf{\Lambda}_1 \mathbf{P} \mathbf{L}_2 \mathbf{\Lambda}_2\| > 0$. Since g belongs to the sector $[0, \mu]$, with $\mu > 0$, it can be verified that $x/g(x) \geq 1/\mu$, $\forall x \in \mathbb{R}$, and we can bound \dot{V} by

$$\dot{V} \leq c \|\mathbf{g}_1(\boldsymbol{\phi}_1)\| \cdot \|\mathbf{g}_2(\boldsymbol{\kappa})\| - \frac{\delta \lambda_{m_2}}{\mu} \|\mathbf{g}_2(\boldsymbol{\kappa})\|^2 - \frac{q_m}{2} \|\mathbf{g}_1(\boldsymbol{\phi}_1)\|^2$$

Choosing $\delta \geq \mu([c/\sqrt{2q_m}]^2 + \alpha)/\lambda_{m_2}$, where $\alpha > 0$, gives

$$\begin{aligned} \dot{V} &\leq -\left(\frac{c}{\sqrt{2q_m}} \|\mathbf{g}_2(\boldsymbol{\kappa})\| - \sqrt{\frac{q_m}{2}} \|\mathbf{g}_1(\boldsymbol{\phi}_1)\|\right)^2 - \alpha \|\mathbf{g}_2(\boldsymbol{\kappa})\|^2 \\ &\triangleq -W(\mathbf{g}_1(\boldsymbol{\phi}_1), \mathbf{g}_2(\boldsymbol{\kappa})). \end{aligned} \quad (82)$$

The function W is a positive definite function of $\mathbf{g}_1(\boldsymbol{\phi}_1)$ and $\mathbf{g}_2(\boldsymbol{\kappa}) = \mathbf{g}_2(\mathbf{M}_3 \boldsymbol{\phi}_2)$. Noting that $g(x) = 0$ if and only if $x = 0$ and that matrix \mathbf{M}_3 has full column rank we can conclude that $W = 0$ if and only if $\boldsymbol{\phi}_1 = \mathbf{0}$ and $\boldsymbol{\phi}_2 = \mathbf{0}$. Hence, W is a positive definite function of $\boldsymbol{\phi}_1$ and $\boldsymbol{\phi}_2$. Consequently the origin of the nominal system (79) is GAS and since (79) is time-invariant, the origin is UGAS. This result is equivalent to that in [18].

Although the Lyapunov function (80) has made it possible to prove UGAS for the origin of (79), and it satisfies (40), it does not satisfy (41). However, as shown in [18] the function $\tilde{V} \triangleq \ln(V+1)$ satisfies both (40) and (41), since

$$\dot{\tilde{V}} \leq -\frac{1}{V(\boldsymbol{\phi})+1} W(\mathbf{g}_1(\boldsymbol{\phi}_1), \mathbf{g}_2(\mathbf{M}_3 \boldsymbol{\phi}_2)) \triangleq -\tilde{W}(\boldsymbol{\phi}) < 0, \quad (83)$$

satisfies (40) and

$$\left\| \frac{\partial \tilde{V}}{\partial \boldsymbol{\phi}} \right\| \leq \frac{1}{V+1} (\delta \|\boldsymbol{\phi}_2\| + \|\mathbf{g}_1(\boldsymbol{\phi}_1)\| \cdot \|\mathbf{P}\|) \quad (84)$$

$$\leq \delta \frac{\|\boldsymbol{\phi}_2\|}{\frac{1}{2} \|\boldsymbol{\phi}_2\|^2 + 1} + \|\mathbf{g}_1(\boldsymbol{\phi})\| \cdot \|\mathbf{P}\| \leq C_1, \quad C_1 > 0, \quad (85)$$

satisfies (41), where we used that $\|\mathbf{g}_1(\boldsymbol{\phi})\|$ is globally bounded.